Insulin-like growth factor binding protein-1 improves vascular endothelial repair in the setting of insulin resistance

Amir Aziz*[1], Natalie J Haywood*[1], Paul A Cordell,[1] Jess Smith[1], Nadira Y Yuldasheva[1], Anshuman Sengupta[1], Noman Ali[1], Ben N Mercer[1], Romana S Mughal[1], Kirsten Riches[2], Richard M Cubbon[1], Karen E Porter[1], Mark T Kearney[1], Stephen B Wheatcroft[1]

*These authors contributed equally to the manuscript

[1]Leeds Institute of Cardiovascular and Metabolic Medicine and Multidisciplinary Cardiovascular Research Centre, University of Leeds, UK

[2]School of Medical Sciences, University of Bradford, UK

Short title: IGFBP1 and endothelial repair

Keywords: Insulin resistance, Animal Models of Human Disease, Growth Factors/Cytokines, Pathophysiology, Vascular Biology

Address for correspondence and reprint requests: Dr Stephen B Wheatcroft, Division of Cardiovascular & Diabetes Research, Leeds Institute of Cardiovascular and Metabolic Medicine and the Multidisciplinary Cardiovascular Research Centre, LIGHT Laboratories, Clarendon Way, University of Leeds, Leeds, LS2 9JT, UK.

Email: s.b.wheatcroft@leeds.ac.uk

Funding: This work was funded by a British Heart Foundation Clinical Research Training Fellowship for AA. RMC holds a British Heart Foundation Intermediate Clinical Research Fellowship. MTK holds a British Heart Foundation Chair in Cardiology. SBW holds a European Research Council Starting Grant.

Disclosure statement: the authors have nothing to disclose.

Abstract

Insulin resistance is associated with impaired endothelial regeneration in response to mechanical injury. We recently demonstrated that insulin-like growth factor binding protein-1 (IGFBP1) ameliorated insulin resistance and increased nitric oxide generation in the endothelium. In this study, we hypothesised that IGFBP1 would improve endothelial regeneration and restore endothelial reparative functions in the setting of insulin resistance. In mice heterozygous for deletion of insulin receptors ($IR^{+/-}$), endothelial regeneration after femoral artery wire injury was enhanced by transgenic expression of human IGFBP1. This was not explained by altered abundance of circulating myeloid angiogenic cells. Incubation of human endothelial cells with hIGFBP1 increased integrin expression and enhanced their ability to adhere to and repopulate denuded human saphenous vein *ex vivo*. *In vitro*, induction of insulin resistance by TNFα significantly inhibited endothelial cell migration and proliferation. Co-incubation with hIGFBP1 restored endothelial migratory and proliferative capacity. At the molecular level, hIGFBP1 induced phosphorylation of focal adhesion kinase, activated RhoA and modulated TNFα-induced actin fibre anisotropy. Collectively, the effects of hIGFBP1 on endothelial cell responses and acceleration of endothelial regeneration in mice indicate that manipulating IGFBP1 could be exploited as a putative strategy to improve endothelial repair in the setting of insulin resistance.

Précis

IGFBP1 ameliorated insulin resistance-induced defects in re-endothelialization *in vivo* and impairment of endothelial migration and proliferation *in vitro* via FAK and RhoA activation.

Introduction

Functional and structural integrity of the endothelial monolayer plays a critical role in vascular homeostasis. Damage to the endothelium by exposure to vascular risk factors or mechanical trauma predisposes to a range of pathologies including atherosclerosis (1), bypass graft failure (2), restenosis (3) and stent thrombosis (4). Regeneration of damaged endothelium following injury is essential to prevent adverse remodelling and is mediated by two broad mechanisms: proliferation and migration of local endothelial cells (5,6) and recruitment of circulating cells to the injured vessel (7). The latter include endothelial colony forming cells (ECFC) which are fully committed to the endothelial lineage and can form mature vascular networks; and myeloid angiogenic cells (MAC) which exhibit a macrophage/monocyte-like phenotype and contribute to endothelial repair through the secretion of pro-angiogenic cytokines (8).

Type 2 diabetes mellitus is associated with both dysfunctional vascular endothelial regeneration and a high risk of cardiovascular events. Insulin resistance has emerged as a major player in diabetes-related vasculopathy, not least through its strong association with endothelial dysfunction (9). Although diabetes is strongly associated with defective vascular repair, we identified that insulin resistance *per se* is sufficient to jeopardise endothelial regeneration after arterial injury (10). Endothelial regeneration following mechanical wire-induced arterial injury was impaired in mice heterozygous for deletion of the insulin receptor ($IR^{+/-}$) - explained at least in part through reduced mobilisation of MACs (10). Recognition of the adverse impact of insulin resistance on endothelial repair processes led us to question whether insulin sensitization might enhance endothelial regeneration in the setting of insulin resistance.

Insulin-like growth factor binding protein-1 (IGFBP1) is one of a family of circulating proteins which confer spatial and temporal regulation of IGF bioavailability but which can also orchestrate cellular responses independent of their modulation of IGF actions (11). At the structural level, IGF-independent actions of IGFBP1 have been ascribed to an Arg-Gly-Asp

(RGD) motif within its C-terminal domain which can interact with cell surface integrins and promote migratory responses in certain cell types (12,13). However, potential effects of IGFBP1 on migratory responses have not previously been studied in endothelial cells.

From the functional perspective, an inhibitory effect of insulin on hepatic IGFBP1 synthesis has led to IGFBP1 being implicated in glucose regulation (14). The circulating concentration of IGFBP1 has been proposed as a biomarker of insulin sensitivity (15,16). In epidemiological studies, low plasma IGFBP1 concentrations are strongly predictive of the prospective development of type 2 diabetes (17–19). We recently identified direct actions of the RGD-domain of IGFBP1 in augmenting insulin signalling and insulin-stimulated glucose uptake (20). Human studies also indicate a link between low circulating IGFBP1 concentration and risk of cardiovascular disease (16,21). Conversely, in the setting of acute myocardial infarction IGFBP1 levels predict mortality but the effect may be confounded by association with elevated levels of co-peptin (22,23).

We have demonstrated in preclinical studies that IGFBP1 plays a favourable role in both insulin sensitivity and vascular function (24). Transgenic expression of human IGFBP1 in mice was associated with whole-body and vascular insulin sensitization, increased basal nitric oxide (NO) bioavailability, lower blood pressure and reduced susceptibility to atherosclerosis (24).

Here we hypothesised that increasing the concentration of IGFBP1 would ameliorate the detrimental effects of insulin resistance on endothelial repair. To investigate this, we assessed endothelial regeneration in $IR^{+/-}$ mice expressing human IGFBP1 subjected to arterial injury and evaluated the effects of hIGFBP1 on the functional properties of endothelial cells *in vitro*.

Material and Methods

Chemicals and antibodies

The antibodies used for immunoblotting are listed in Table 1. Chemicals were purchased from Sigma Chemical/Sigma-Aldrich (St. Louis, MO), unless otherwise specified. Human IGFBP1 and IGF-1 were purchased from GroPep (Adelaide, Australia). Recombinant hIGFBP1 was expressed in Expi293F cells (Life Technologies) using the SUMOStar expression system (LifeSensors) and purified as described previously (20). Site-directed mutagenesis of the hIGFBP-1expressing plasmid was performed using the QuikChange Lightning kit (Agilent Technologies) using primers 5′-TCCAGAGATCTGGGGAGACCC-3′ and 5′-GGGTCTCCCCAGATCTCTGGA-3′ to generate the WGD hIGFBP1 expression construct.

Animals.

$IR^{+/-}$ mice (25) were bred in house from founder animals originating from the Medical Research Council Mammalian Genetics Unit (Harwell, Oxfordshire, U.K.). hIGFBP1 transgenic (tg) mice were originally generated by Crossey et al at King's College London (26), and subsequently backcrossed to a C57BL/6J background for multiple generations. $IR^{+/-}$ and hIGFBP1 mice were inter-crossed to generate $IR^{+/-}hIGFBP1_{tg}$ mice. Animals were maintained as heterozygotes on a C57BL/6 background in a conventional animal facility with a 12-h light/dark cycle and received a standard laboratory diet. Male WT, $IR^{+/-}$, $hIGFBP1_{tg}$, and $IR^{+/-}hIGFBP1_{tg}$ littermate mice (aged 12–16 weeks) were compared. Genotyping was performed using PCR on ear notch genomic DNA, with the primers described previously (24,27). All procedures were approved by the Animal Welfare and Ethical Review Committee at the University of Leeds and were carried out in accordance with the Animals (Scientific Procedures) Act 1986 Amendment Regulations 2012.

Plasma IGFBP1 concentration

Circulating concentration of IGFBP1 was measured in plasma of non-fasted animals using a commercially available ELISA kit according to the manufacturer's instructions (IGFBP1 ELISA kit ab100539, Abcam, Cambridge, UK).

Vascular injury.

Mice were anaesthetised with isoflurane (2.5–5%) before a small incision was made in the mid-thigh to permit isolation of the femoral artery (28). Following an arteriotomy made using iris scissors (World-Precision Instruments, Sarasota, FL), a 0.014-inch-diameter angioplasty guide wire with tapered tip (Hi-torque Cross-it XT, Abbott-Vascular, Abbott, IL), was introduced. The angioplasty guide wire was advanced 3cm, and three passages were performed per mouse, resulting in complete arterial denudation. The guide wire was removed and the suture was tightened rapidly. The vessel was then ligated, and the skin was closed with a continuous suture. The contralateral artery underwent an identical sham operation, without passage of the wire. Animals received postoperative analgesia with buprenorphine (0.25 mg/kg).

Assessment of endothelial regeneration by *en face* microscopy.

Mice were anesthetized five days after wire injury, and 50 µL of 0.5% Evans blue dye injected into the inferior vena cava. The mice were perfused/fixed with 4% paraformaldehyde in PBS before the femoral arteries (injured and uninjured) were harvested. The vessels were opened longitudinally. The areas stained and unstained in blue were measured in a 5mm injured segment beginning 5mm distal to the aortic bifurcation, and the percentage areas were calculated using ImageProPlus7.0 software (Media Cybernetics, Bethesda, MD).

Mononuclear cell isolation and culture.

Isolation of mononuclear cells (MNCs) from 1 mL of blood, obtained from the vena cava under terminal anaesthesia, was by Histopaque-1083 (Sigma) density gradient centrifugation. MNCs were seeded on fibronectin 24-well plates (BD Biosciences) at a density of 1×10^6 cells/well.

Cells were cultured in EC growth (EGM-2) medium supplemented with EGM-2 Bullet kit (Lonza, Basel, Switzerland) in addition to 20% FCS.

Spleens obtained from mice under terminal anaesthesia were minced mechanically. MNCs were isolated by density gradient centrifugation, as described above. After washing steps, cells were seeded on fibronectin 24-well plates at a seeding density of 8×10^6 cells/well and cultured as described above.

Tibias and femurs were flushed three times in DMEM with a 26-gauge needle to collect bone marrow (BM). MNCs were isolated by density gradient centrifugation as described above. After washing steps, cells were seeded on fibronectin 24-well plates at a seeding density of 1×10^6 cells/well and cultured as described above.

Myeloid Angiogenic Cell characterization.

After four days incubation at 37°C in 5% CO_2, gentle washing with PBS discarded non-adherent cells and adherent cells were re-suspended in medium. At day 7, attached cells from peripheral blood, spleen, and BM were stained for the uptake of 1,1'-dioctadecy-3,3,3′,3′-tetramethyllindocarbocyanine-labeled acetylated low-density lipoprotein (DiI-Ac-LDL) (Molecular Probes, Invitrogen, Carlsbad, CA) and lectin from *Ulex europaeus* FITC conjugate (Sigma). Cells were first incubated with DiI-Ac-LDL at 37°C for 3h and later fixed with 4% paraformaldehyde for 10 minutes. Cells were washed and reacted with lectin for 1h. After staining, cells were quantified by examining 10 random high-power fields (HPF) and double-positive cells were identified as MACs.

MAC function: adhesion assay.

To assess adhesion, 50,000 MACs were re-suspended in EGM-2 medium, plated onto 24-well plates coated with indicated substrates, and incubated for 1 h at 37°C. After washing three times with PBS, attached cells were counted. Adhesion was evaluated as the mean number of attached cells per HPF (×100).

Fluorescence-activated cell sorter enumeration of Sca-1/Flk-1 cells.

Murine saphenous vein blood samples (100µL) were incubated with PharmLyse (BD Biosciences, San Jose CA) at room temperature. After centrifugation, mononuclear cells (MNCs) were re-suspended in fluorescence-activated cell sorter (FACS) buffer and incubated with FcR blocker (BD Biosciences) at 4°C. As per protocol, appropriate volumes of the antibodies, or their respective isotype controls, were added for 10 minutes at 4°C: fluorescein isothiocyanate (FITC) anti-mouse Sca-1 and PE anti-mouse Flk-1 (BD Biosciences). Enumeration of APCs was performed using flow cytometry (BD FACS Calibur) to quantify dual-stained Sca-1/Flk-1 cells. Isotype control specimens were used to define the threshold for antigen presence and to subtract non-specific fluorescence. The cytometer was set to acquire 100,000 events within the lymphocyte gate, defined by typical light scatter properties.

***Ex-vivo* Saphenous vein adhesion assay**

Saphenous vein segments were obtained from patients undergoing coronary artery bypass graft surgery at Leeds Teaching Hospitals NHS Trust, Leeds, UK following ethical approval. Human coronary artery endothelial cells (HCAECs) (Promocell, Heidelberg, Germany) stained with CellTracker CM-DiI (Invitrogen, Oregon, USA) were incubated for one hour at a fixed density (250,000 cells/ml) in full (20%) ECGM suspension with either control vehicle or hIGFBP1 (500ng/mL) (GroPep, Australia). After one hour, 50,000 cells from each treatment group were seeded onto a denuded segment of human saphenous vein and incubated for 5 minutes. After 5 minutes, the cell suspension was gently washed with PBS, Hoecht stain was then added to the saphenous vein segment and finally re-suspended in full (20%) ECGM. Images were obtained by confocal microscopy of the vein segments, assessing the number of cells adhering to the saphenous vein matrix.

Endothelial cell adhesion assays

The potential for hIGFBP1 to modulate adhesion was investigated in adhesion assays performed with HCAECs. HCAEC suspensions (100,000 cells/mL) were seeded onto sterile

glass cover slips. Vehicle-treated wells contained 1% FCS and treatment wells contained hIGFBP1 (500ng/mL in 1% FCS). Adherent cells in one vehicle-treated well and one corresponding IGFBP-1 well were fixed after 2 hours, 4 hours and 6 hours of incubation at 37°C in 4% paraformaldehyde and stained with Haematoxylin & Eosin for 1 minute. Finally, the cover slips were mounted onto microscope slides using glycerol gelatin and 10 random fields containing the adherent cells were counted at 400x magnification.

To investigate the potential for hIGFBP1 to modulate adhesion to individual extracellular matrix components, HUVECS were seeded at 50,000 cells per well of 24 well plates coated with fibronectin (Corning, 354411), collagen I (Thermo fisher Scientific, A1142802), collagen IV (Corning, 734-0127) or vitronectin (coated in house, using Novoprotein, C395 at 1µg/well). and incubated for 30mins at 37°C. Cells were washed once with PBS and attached cells were counted. Adhesion was evaluated as the mean number of attached cells per HPF (×40). The involvement of focal adhesion kinase (FAK) was investigated using the FAK inhibitor PZ0117 (Sigma-Aldrich; 100 nmol/L).

Integrin-Mediated Cell Adhesion

Cell surface subunit or heterodimer integrins were quantified using an integrin-mediated cell adhesion array kit (ECM532, Millipore). HCAECs were grown to confluence in T-75 flasks. Once confluent, cells were harvested using Gibco® Cell Dissociation Buffer. HCAECs were co-incubated with or without hIGFBP1 (500ng/mL) for one hour before 100,000 cells were added to the integrin antibody-coated and control wells and incubated for 2h at 37°C. Unbound cells were then washed off and the adherent cells stained. The optical density of nuclear stain extracts was measured at 540nm (OD540nm) on a MRX TC 2 microplate reader (DYNEX Technologies, U.K.).

Migration assays

Migration of HCAECs and Human Umbilical Vein Endothelial Cells (HUVECs) was investigated in twelve-well plates using a modification of a 'scratch wound' method. Briefly, duplicate scratches were made with a sterile 1 ml pipette tip in confluent endothelial monolayers (having been quiesced in medium containing 1% FBS for 16h), reference points etched in the dishes and images were captured (0h). Cells were then exposed to hIGFBP1 (500ng/mL), TNF-alpha (10ng/mL) or both in combination with 10% FBS endothelial cell growth medium in a tissue-culture incubator for an additional 48h. Further images were then captured by aligning the dishes with the reference point made at time 0h, and images were acquired at 24h and 48h. Quantification was achieved by counting the number of cells which had migrated beyond a fixed distance from the initial wound edge.

Endothelial cell migration was also studied using a modified Boyden chamber technique, as we have described previously (29). HCAECs or HUVECS (100,000) were loaded in the upper chamber in medium supplemented with 20% FBS. The lower chamber contained 20% FBS with hIGFBP1 (500ng/mL) or VEGF (50ng/mL). After incubation for 6 h at 37°C in a tissue-culture incubator, duplicate membranes were processed and evaluated by counting migrated cells on the underside of the membrane in 10 random fields under high power (×400) light microscopy.

Cell proliferation assays

HCAEC and HUVEC proliferation assays were performed by seeding cells in 24-well culture plates at a density of 20,000 cells per well in full endothelial growth medium (20% FBS). After 30-32h, incubated cells were quiesced in medium containing 1% FBS for 16 hours. Cells were then exposed to control growth medium (20% FBS) and hIGFBP1 (500ng/mL), TNF-alpha (0.1ng/mL) or both in combination. Medium and chemicals were replaced on days 2 and 4

and viable cell number determined in triplicate wells on day 5 using Trypan Blue and a haemocytometer. In additional experiments, proliferation was assessed in HUVEC by an EdU (5-ethynyl-2'-deoxyuridine) kit in accordance with the manufacturer's instructions (Click-iT EdU Alexa Fluor 488 Imaging Kit; C10337; Invitrogen). The proliferative response to hIGFBP1 (500ng/mL) +/- IGF-1 (18nmol/L) (Gropep, Adelaide, Australia) were studied. Involvement of focal adhesion kinase (FAK) was investigated using the FAK inhibitor PZ0117 (Sigma-Aldrich; 100 nmol/L).

Western blotting for p-FAK and p-Akt

HUVEC after four hours of serum-starvation were incubated +/- hIGFBP1 or WGD-hIGFBP1 (500ng/mL) for 15 minutes. Protein was extracted in lysis buffer and quantified using the protein BCA assay (Sigma-Aldrich). Then, 30µg of protein were separated by electrophoresis through 4–12% SDS-PAGE gels (Invitrogen Life Technologies, Carlsbad, CA) and blotted onto polyvinylidene fluoride membranes. Immunoblots were performed as previously (30) described using antibodies listed in Table 1. Inhibition by TNF-α of insulin-stimulated Akt phosphorylation was determined in HUVEC. Cells were incubated with TNF-α (10ng/mL) for the indicated durations (30-120 mins) and then stimulated with insulin (100nmol/L 15 mins) to assess the effects of TNF-α on insulin-induced Akt phosphorylation.

RhoA activity assay

HCAECs were seeded at 100,000 cells/well into 6 well plates. On reaching 80% confluence cells were serum starved overnight and then treated with hIGFBP1 for the following times: 0 minutes, 10 minutes, 20 minutes and 40 minutes. After treatment, the medium was aspirated and washed thrice with ice-cold PBS being especially careful to remove all residual PBS. Cells were then lysed with 120 µL of ice-cold lysis buffer (1:100 of Protease inhibitor:lysis buffer), harvested and transferred into microcentrifuge tubes on ice. The samples were centrifuged at 10,000g, 4 °C for 2 minutes. 20µL of lysate were taken off and stored at 4 °C for protein

quantification and the remainder used to assess RhoA activity assay by the RhoA G-LISA kit (Cytoskeleton, Inc., Denver, Colorado, USA) according to the manufacturer's instructions.

Endothelial cell actin fibre anisotropy assessment

HCAECs were seeded at 12,000 cells/well in gelatin-coated Labtek 8-well chamber slides then grown for 48h in ECGM/20% FCS. Subsequently cells were incubated for 24h in ECGM/10%FCS alone or with either hIGFBP1 (500ng/mL), TNF-α (10ng/mL Peprotech) or both proteins. Prior to fixation, cells were washed once with PBS at 37ºC then treated with 3% paraformaldehyde in PBS (warmed to 37ºC) for 20 min. To remove unreacted paraformaldehyde, cells were washed three times with PBS, incubated for 10 min with 50mM NH_4Cl in PBS then washed three further times with PBS. Prior to staining, cells were permeabilised for 4 minutes with 0.2% triton X 100 in PBS followed by three PBS washes, then blocked for 30 minutes with 0.2% fish skin gelatin in PBS (FSG/PBS). Actin filaments were stained with FITC-phalloidin (Enzo Life science) at 1.5 ug/ml final concentration in FSG/PBS for 1h followed by 3 washes with FSG/PBS, one wash in PBS and one wash in deionized water. Cells were mounted with Duolink In Situ Mounting Medium with DAPI (Sigma) and actin filaments and cell nuclei were imaged on Delta Vision widefield deconvolution system (Applied Precision), and Zeiss LSM 700 laser-scanning confocal microscopes. On the Delta Vision microscope images were acquired with a 40x 1.35NA oil objective at 0.2 µm z-intervals at 1024x1024 pixel resolution images were processed with 10 cycles of deconvolution (conservative model) before generation of an 8-bit maximum intensity projection for analysis. On the LSM700 microscope images were acquired with a 40x1.3NA oil objective and were scanned at 1024x1024 pixel resolution at 8-bits per pixel. Optical section thickness was set at 1 Airy unit and z-step at 0.48 µm.

The Fibril Tool plug-in for Image J (31) was used to analyse the anisotropy of actin fibres in FITC-phalloidin images. Whole cells with intact nuclei were included in the analysis. Cells were subdivided into 2-8 sub-regions (corresponding to major fibre cluster alignments and avoiding

the nucleus and saturated areas) using the polygon tool and anisotropy for each cell was calculated as an area- weighted average of sub-regions.

Data analysis

Results are expressed as mean±SEM. Data were demonstrated to be normally distributed using the Shapiro-Wilk test. Comparisons within groups were made using paired Students t-tests and between groups using unpaired Students t tests or repeated measures ANOVA with post-hoc Newman-Keuls tests, as appropriate. $P<0.05$ was considered statistically significant.

Results

Transgenic expression of hIGFBP1 ameliorates the detrimental effects of insulin resistance on endothelial regeneration.

Endothelial regeneration was quantified in murine femoral arteries five days after wire-induced arterial injury, which we determined as the time-point at which re-endothelialisation was maximally impaired in insulin resistant mice (10). There was no difference in endothelial regeneration between $hIGFBP1_{tg}$ and wild type animals [Fig 1A&B]. As whole body metabolic phenotype is not altered in hIGFBP1tg mice (24) this indicates that increasing hIGFBP1 does not alter endothelial regeneration in metabolically normal animals. In contrast, impaired endothelial regeneration observed in $IR^{+/-}$ mice was significantly improved by overexpression of hIGFBP1 [Fig 1 A&C]. Plasma concentration of IGFBP1 was significantly increased in $hIGFBP1_{tg}$ mice and was similarly increased in insulin resistant $IR^{+/-}$ mice overexpressing hIGFBP1 (supplementary fig 1).

Enhanced endothelial regeneration in hIGFBP1 expressing insulin resistant mice is not attributable to changes in abundance or function of circulating angiogenic progenitor cells.

Endothelial regeneration following mechanical injury is accomplished by an orchestrated cellular response comprising the proliferation and migration of vessel-wall resident endothelial cells and the recruitment of circulating cells with angiogenic potential (7). We have previously reported that impaired endothelial regeneration in $IR^{+/-}$ mice is associated with reduced abundance of circulating MACs, and decreased mobilisation of $Sca\text{-}1^{+}/Flk\text{-}1^{+}$cells from bone marrow (10). We therefore investigated whether changes in abundance of MACs were responsible for enhanced endothelial regeneration in mice expressing hIGFBP1 in the current study. We found no difference between WT and $hIGFBP1_{tg}$ mice in abundance of blood-derived MACs (fig 2A). The yield of circulating MACs was reduced in $IR^{+/-}$ mice but was not significantly modified by the expression of hIGFBP1 (fig 2A). The yield of MACs from bone-marrow and spleen was similar in all groups of mice (fig 2B-C). Adhesion of MACs to fibronectin-coated plates was uninfluenced by genotype (fig 2D). The abundance of

Sca-1^+/Flk-1^+ cells in the mononuclear cell fraction of blood was measured by flow cytometry and was similar in all groups of mice (fig 2E).

Acute exposure to hIGFBP1 increases adherence of human endothelial cells to human vessels and upregulates availability of integrins.

To examine whether hIGFBP1 directly modulates the reparative function of native endothelial cells, we first examined the effects of short term incubation with hIGFBP1 on the adhesive properties of endothelial cells. We investigated the ability of human coronary artery endothelial cells (HCAEC) to adhere to endothelium-denuded segments of human saphenous vein. We found that HCAEC were adherent to denuded saphenous vein after five minutes (fig 3A). Pre-incubation with hIGFBP1 (500ng/mL 1 hour) resulted in a significant increase in the number of adherent cells (fig 3B-C). In contrast to the modulatory effect of hIGFBP1 on adhesion to a denuded vessel, incubation with hIGFBP1 had no effect on adhesion of HCAEC to uncoated glass coverslips (fig 3D). Because adhesion of endothelial cells to extracellular matrix is critically dependent on interaction of matrix components (e.g. fibronectin) with cell surface integrins (32), we quantified functional integrin abundance using an integrin-mediated cell adhesion array kit. We found that incubation of HCAEC with hIGFBP1 (500ng/mL 1 hour) lead to significant increase in the cell surface abundance of α_2 and α_V integrin subunits and of $\alpha_V\beta_3$ and $\alpha_5\beta_1$ integrins (fig 3E-F). To further characterise the upregulation of endothelial cell adhesion by hIGFBP1, we investigated the effects of hIGFBP1 on adherence of HUVEC to individual extracellular matrix (ECM) components *in vitro*. There was a trend to increased adhesion on several matrices but we were not able to identify a dominant ECM constituent to which hIGFBP1 preferentially increased adhesion (supplementary fig 2).

hIGFBP1 ameliorates insulin-resistance induced endothelial migratory and proliferative defects in human endothelial cells

Regeneration of injured endothelium by local resident endothelial cells is dependent on their ability to migrate and proliferate to form a neo-endothelium. In linear wound assays, we

found that incubation with hIGFBP1 (500ng/mL; 1 hour) did not influence migration of either human umbilical vein endothelial cells (HUVEC) or HCAEC (fig 4A-B). To mimic the biochemical milieu to which endothelial cells are exposed in insulin resistant states *in vivo*, we pre-incubated HUVEC with tumor necrosis factor (TNF)-α to inhibit the insulin signaling pathway (fig 4C-D). Incubation with TNF-α (10ng/mL) inhibited migration of HUVEC (fig 4E) and HCAEC (fig 4F), which was ameliorated in both types of endothelial cell by co-incubation with hIGFBP1 (500ng/mL) (fig 4E-F). We also investigated whether hIGFBP1increased migration of endothelial cells in a modified Boyden chamber assay. There was no difference in migration of HUVEC or HCAEC indicating that hIGFBP1 does not act as a chemotactic stimulus for endothelial cells (fig 5A-B). Similarly, hIGFBP1 did not modulate the migratory response of HCAEC to the potent chemotactic stimulus vascular endothelial growth factor (fig 5C).

In both HUVEC and HCAEC, incubation with hIGFBP1 led to a trend to increased cell proliferation assessed by cell counting which did not reach statistical significance (fig 6A-B). Incubation with TNF-α inhibited proliferation of HCAEC in a concentration-dependent manner (fig 6C). The anti-proliferative effects of TNF-α were ameliorated by incubation of HCAEC with hIGFBP1 (fig 6D).

Pro-reparative effects of hIGFBP1 on the endothelium are dependent on its RGD domain and focal adhesion kinase.

To further explore the molecular basis of the pro-reparative effects of hIGFBP1 in the endothelium, we employed an EdU assay to quantify the effects of hIGFBP1 on proliferative responses in HUVEC. We found a significant dose-dependent increase in cell proliferation at hIGFBP1 concentrations of 100-500ng/mL (Supplementary fig 3). As IGFBPs are known to act variably as IGF-modulators or independently of IGF contingent on context, we next compared the effects of IGF-1 and hIGFBP1 on endothelial cell proliferation. Equimolar concentrations of IGF-1 and hIGFBP1 both individually stimulated proliferation to a similar extent, but there was no evidence of an additive effect (fig 7A). We then mutated the RGD

domain of IGFBP1, responsible for binding to cell surface integrins, to a non-functional WGD domain incapable of integrin binding (20). Stimulation of endothelial cell proliferation by hIGFBP1 was ameliorated by RGD -> WGD mutation (fig 7B&C). Focal adhesion kinase (FAK) is an important signalling node downstream of integrins and is known to mediate proangiogenic signalling in endothelial cells (33). Inhibition of FAK abrogated the stimulatory effect of hIGFBP1 on cell proliferation (Figure 7D) and reduced adhesion to collagen IV in the presence of hIGFBP1 (suppl fig 2F).

Acute exposure to hIGFBP1 leads to phosphorylation of focal adhesion kinase, activation of RhoA and modulation of F-actin organisation in endothelial cells.

Because the RGD motif of hIGFBP1 is capable of interaction with cell-surface integrins, we investigated whether hIGFBP1 activates outside-in integrin-mediated signalling in endothelial cells. We found that incubation of HUVEC with hIGFBP1 led to acute phosphorylation of the critical integrin signalling intermediary FAK (fig 8A-B). The non-integrin binding WGD mutant hIGFBP1 had no effect on FAK phosphorylation (fig 8C-D). Endothelial cell migration is dependent on cytoskeletal rearrangements in which the small GTPase RhoA plays a critical role (34). We observed rapid time-dependent activation of RhoA in HUVEC in response to hIGFBP1 (fig 8E). The cytoskeletal rearrangements associated with endothelial cell motility are complex, involving formation and dissolution of focal adhesions and the remodelling of actin filaments. We assessed cytoskeletal remodelling by quantifying actin filament anisotropy. Incubation with TNF-α led to a significant increase in actin filament anisotropy which was inhibited by co-incubation with hIGFBP1 (fig 8 F-G).

Discussion

This study demonstrated that transgenic expression of hIGFBP1 partially reversed the endothelial regenerative dysfunction in insulin resistant $IR^{+/-}$ mice. This was not explained by modulation of the abundance or function of MACs which are known to be impaired in $IR^{+/-}$ mice (10). *In vitro*, we observed favourable effects of hIGFBP1 on multiple endothelial cell functional properties integral to endothelial regeneration, including increased adhesion to extracellular matrix and amelioration of the detrimental effects of insulin resistance on proliferative and migratory responses. At the molecular level, hIGFBP1 induced integrin signalling through rapid phosphorylation of FAK, increased activity of the small GTPase RhoA and modulated the effects of the pro-inflammatory cytokine TNF-α on cytoskeletal remodelling in endothelial cells. Collectively, these findings add further support to the emerging concept of a vasculo-protective role for IGFBP1 and raise the possibility that increasing IGFBP1 concentration may be a strategy to improve endothelial repair in insulin resistant states.

Damage to the vascular endothelium can result from diverse insults including exposure to the adverse biochemical milieu associated with the presence of vascular risk factors or mechanical trauma associated with surgical or percutaneous revascularisation procedures. Endogenous repair mechanisms, which mitigate against the development of atherosclerosis, thrombosis and restenosis, are deficient in the presence of diabetes (35). We previously reported that endothelial regeneration following arterial injury was impaired in insulin resistant mice ($IR^{+/-}$), in which reduced NO bioavailability and defective mobilisation of MACs from bone marrow contributed to the reduced abundance of circulating MACs (10). In a separate study, we reported that hIGFBP1 improved vascular insulin sensitivity and increased vascular NO bioavailability in $IR^{+/-}$ mice (24). Intriguingly, the enhanced repair observed in $IR^{+/-}$ mice expressing hIGFBP1 in the current study was not explained by changes in the abundance or adhesive properties of circulating MACs. Although we cannot exclude the possibility of changes in other classes of circulating progenitor cells, our data

suggest that effects of hIGFBP1 on local endothelial cells *per se* may predominate in the modulation of endothelial repair. In keeping with this suggestion, the contribution of circulating progenitor cells to endogenous endothelial regeneration has been drawn in to question (36,37), reigniting interest in the long-recognised contribution of local, mature endothelial cells to endothelial repair (5,6,38).

Circulating concentrations of IGFBP1 have been associated with both metabolic regulation and cardiovascular disease. In non-diabetic humans, low levels of IGFBP1 are predictive of the subsequent development of diabetes (17–19). However, data linking IGFBP1 levels with cardiovascular disease development are conflicting (15,22,23) It is, therefore, important to address whether IGFBP1 directly impacts on the function of vascular cells. We observed a significant increase in plasma IGFBP1 levels in hIGFBP1-transgenic mice which was similarly increased in $IR^{+/-}$ mice overexpressing hIGFBP1. The levels achieved in $hIGFBP1_{tg}$ mice in the current dataset are around two-fold higher than circulating levels in healthy non-obese humans (39), and are substantially higher than those in obese C57BL6 mice (24).

IGFBP1 is known to modulate migratory and/or proliferative responses in a range of cell types, predominantly through interaction of the RGD sequence within its C-terminal domain with $\alpha_5\beta_1$ integrin (12,13,40–42)In keeping with a critical impact of the RGD sequence of IGFBP1 on diverse cellular responses, we recently demonstrated that hIGFBP1 directly modulates insulin signalling and insulin-stimulated glucose uptake in skeletal muscle cells through an RGD-dependent mechanism (20). However, this is the first study to report a modulatory effect of IGFBP1 on functional responses in endothelial cells. Several fundamental actions pertinent to endothelial repair, including adhesion, migration and proliferation were favourably modulated by hIGFBP1 in this study.

In an *ex-vivo* model of endothelial regeneration, short-term incubation with hIGFBP1 significantly increased the proportion of endothelial cells adherent to endothelium-denuded human saphenous vein. The concentration of hIGFBP1 employed in the cellular experiments was only slightly higher that the levels achieved in the transgenic mice, indicating that

important vascular effects of IGFBP1 can be achieved at physiological or modestly supra-physiological concentrations. In keeping with the key role of integrins in the adhesion of endothelial cells to the extracellular matrix, cell surface expression of integrins $\alpha_V\beta_3$, $\alpha_V\beta_5$ and $\alpha_5\beta_1$ was increased after incubation with hIGFBP1. Interaction of the RGD-motif of IGFBP1 with integrins is well described (12,13), however this is the first time that IGFBP1 has been reported to increase cell surface integrin expression. Although other members of the IGF-binding protein family regulate integrin expression at the transcriptional level (43), the change in cell surface integrin expression observed here is likely to be too rapid to be explained by transcriptional regulation and may reflect recycling of intracellular integrins to the cell membrane (44). *In vitro*, we were unable to identify a dominant ECM component to which hIGFBP1 preferentially increased endothelial cell adhesion. We speculate that the pro-adhesive action we observed in saphenous veins ex vivo is either due to additive minor effects on multiple ECM components or to a selective effect on an ECM constituent we have not selectively studied.

To determine whether a functional RGD domain of IGFBP1 is essential for its stimulatory effects on endothelial repair, we mutated RGD to WGD which is incapable of binding integrins (20). The ability of IGFBP1 to stimulate endothelial cell proliferation and activate downstream signalling pathways was abrogated by loss of a functional RGD domain. The findings of the current study therefore add to the growing body of evidence that the IGFBP1-mediated effects in endothelial cells and skeletal muscle are RGD-integrin mediated.

To mimic insulin resistance *in vitro*, we exposed cells to the cytokine TNF-α. In keeping with previous reports (45,46), TNF-α inhibited migratory and proliferative responses of endothelial cells. Incubation with hIGFBP1 partially restored endothelial migration in a scratch wound assay. However, no effect of hIGFBP1 was evident in the Boyden chamber assay suggesting that hIGFBP1 augments the motility of endothelial cells rather than acting as a chemotactic agent in vascular repair. hIGFBP1 was noted to improve endothelial cell proliferation in the presence of TNF-α.

498 It is notable that the favourable effects of hIGFBP1 on endothelial regeneration in this study
499 were restricted to insulin resistant $IR^{+/-}$ mice with no detectable effect apparent when
500 hIGFBP1 was expressed in insulin sensitive mice. Similarly, modulatory effects of hIGFBP1
501 on endothelial proliferative and migratory responses were apparent *in vitro* only after
502 inducing insulin resistance by incubation with TNF-α. Although it is possible that the pro-
503 reparative effects of hIGFBP1 were attributable to hIGFBP1-mediated insulin sensitization in
504 endothelium, as occurs in skeletal muscle (20), this would not readily explain the modulatory
505 effects of hIGFBP1 observed *in vitro* which were carried out in the absence of exogenous
506 insulin. The failure of hIGFBP1 to improve endothelial regeneration in the insulin sensitive
507 state may, therefore, reflect the fact the reparative processes are already maximal in this
508 setting. How IGFBP1 interacts with endothelial cells at the molecular level remains poorly
509 understood. We demonstrated that IGFBP1 induces nitric oxide generation in endothelial
510 cells independently of IGF by activation of the Akt pathway (24). Other groups have shown
511 that IGFBP1 can activate integrin mediated intra-cellular signalling through its C-terminal
512 RGD sequence and induce migratory or proliferative responses in a range of cell types
513 including Chinese hamster ovary cells (12), oligodendrocytes (13), trophoblast (40), breast
514 cancer cells (41) and schwannoma cells (42). In keeping with activation of downstream
515 integrin signalling by IGFBP1 in the endothelium, we observed rapid RGD-dependent
516 phosphorylation of focal adhesion kinase (FAK), a non-receptor tyrosine kinase, which
517 becomes tyrosine-phosphorylated during integrin-activation and is believed to play a vital
518 role in integrin signal transduction (33,47,48). Inhibition of FAK abrogated the pro-
519 proliferative effects of hIGFBP1. FAK promotes cell migration and angiogenic responses
520 through interaction with a pool of intracellular signaling proteins, including c-Src,
521 phosphatidylinositol 3-kinase (PI3-K), and Rho GTPase family members, which are
522 associated with assembly and disassembly of actin cytoskeleton (49). Coordinated
523 remodelling of actin filaments through dynamic regulation of filament assembly and
524 disassembly is required for endothelial cells to mobilise following vascular injury. In response

to hIGFBP1, we observed rapid and time dependent activation of the small GTPase RhoA which acts as a key player in cytoskeletal rearrangement and endothelial cell migration (34).

Consistent with the known inhibitory effect of TNF-α on actin remodelling and endothelial cell migration (50), we observed a significant increase in actin filament anisotropy following TNF-α stimulation. This was abrogated by co-stimulation with hIGFBP1, providing further evidence that IGFBP1 serves to modulate cytoskeletal remodelling and thereby promote endothelial repair.

In summary, we have demonstrated that IGFBP1 abrogates the inhibitory effects of insulin resistance on endothelial repair *in vivo* and exerts multiple favourable effects on the reparative phenotype of endothelial cells *in vitro*. These findings add to our previous description of insulin-sensitizing and anti-atherosclerotic effects of IGFBP1, are consistent with the argument that low levels of IGFBP1 being permissive for the development of vascular disease and suggest that raising IGFBP1 levels may be an appropriate strategy to promote endothelial repair.

Acknowledgements

a) Acknowledgments: none

b) Sources of Funding: This work was funded by a British Heart Foundation Clinical Research Training Fellowship for AA. RMC holds a British Heart Foundation Intermediate Clinical Research Fellowship. MTK holds a British Heart Foundation Chair in Cardiology. SBW holds a European Research Council Starting Grant.

c) Disclosures: none

References

1. **Dimmeler S, Zeiher AM.** Vascular repair by circulating endothelial progenitor cells: the missing link in atherosclerosis? *J. Mol. Med. Berl. Ger.* 2004;82(10):671–677.

2. **Manchio JV, Gu J, Romar L, Brown J, Gammie J, Pierson RN, Griffith B, Poston RS.** Disruption of graft endothelium correlates with early failure after off-pump coronary artery bypass surgery. *Ann. Thorac. Surg.* 2005;79(6):1991–1998.

3. **Kipshidze N, Dangas G, Tsapenko M, Moses J, Leon MB, Kutryk M, Serruys P.** Role of the endothelium in modulating neointimal formation: vasculoprotective approaches to attenuate restenosis after percutaneous coronary interventions. *J. Am. Coll. Cardiol.* 2004;44(4):733–739.

4. **Finn AV, Joner M, Nakazawa G, Kolodgie F, Newell J, John MC, Gold HK, Virmani R.** Pathological correlates of late drug-eluting stent thrombosis: strut coverage as a marker of endothelialization. *Circulation* 2007;115(18):2435–2441.

5. **Haudenschild CC, Schwartz SM.** Endothelial regeneration. II. Restitution of endothelial continuity. *Lab. Investig. J. Tech. Methods Pathol.* 1979;41(5):407–418.

6. **Itoh Y, Toriumi H, Yamada S, Hoshino H, Suzuki N.** Resident endothelial cells surrounding damaged arterial endothelium reendothelialize the lesion. *Arterioscler. Thromb. Vasc. Biol.* 2010;30(9):1725–1732.

7. **Krankel N, Luscher TF, Landmesser U.** Novel insights into vascular repair mechanisms. *Curr. Pharm. Des.* 2014;20(14):2430–2438.

8. **Medina RJ, Barber CL, Sabatier F, Dignat-George F, Melero-Martin JM, Khosrotehrani K, Ohneda O, Randi AM, Chan JKY, Yamaguchi T, Van Hinsbergh VWM, Yoder MC, Stitt AW.** Endothelial Progenitors: A Consensus Statement on Nomenclature. *Stem Cells Transl. Med.* 2017;6(5):1316–1320.

9. **Kim J, Montagnani M, Koh KK, Quon MJ.** Reciprocal relationships between insulin resistance and endothelial dysfunction: molecular and pathophysiological mechanisms. *Circulation* 2006;113(15):1888–1904.

10. **Kahn MB, Yuldasheva N, Cubbon RM, Surr J, Rashid ST, Viswambharan H, Imrie H, Abbas A, Rajwani A, Aziz A, Baliga V, Sukumar P, Gage M, Kearney MT, Wheatcroft SB.** Insulin resistance impairs circulating angiogenic progenitor cell function and delays endothelial regeneration. *Diabetes* 2011;60(4):1295–1303.

11. **Wheatcroft SB, Kearney MT.** IGF-dependent and IGF-independent actions of IGF-binding protein-1 and -2: implications for metabolic homeostasis. *Trends Endocrinol. Metab. TEM* 2009;20(4):153–162.

12. **Jones JI, Gockerman A, Busby WH, Wright G, Clemmons DR.** Insulin-like growth factor binding protein 1 stimulates cell migration and binds to the alpha 5 beta 1 integrin by means of its Arg-Gly-Asp sequence. *Proc. Natl. Acad. Sci. U. S. A.* 1993;90(22):10553–10557.

13. **Chesik D, De Keyser J, Bron R, Fuhler GM.** Insulin-like growth factor binding protein-1 activates integrin-mediated intracellular signaling and migration in oligodendrocytes. *J. Neurochem.* 2010;113(5):1319–1330.

14. **Lee PD, Giudice LC, Conover CA, Powell DR.** Insulin-like growth factor binding protein-1: recent findings and new directions. *Proc. Soc. Exp. Biol. Med. Soc. Exp. Biol. Med. N. Y. N* 1997;216(3):319–357.

15. **Maddux BA, Chan A, De Filippis EA, Mandarino LJ, Goldfine ID.** IGF-binding protein-1 levels are related to insulin-mediated glucose disposal and are a potential serum marker of insulin resistance. *Diabetes Care* 2006;29(7):1535–1537.

16. **Heald AH, Cruickshank JK, Riste LK, Cade JE, Anderson S, Greenhalgh A, Sampayo J, Taylor W, Fraser W, White A, Gibson JM.** Close relation of fasting insulin-like growth factor binding protein-1 (IGFBP-1) with glucose tolerance and cardiovascular risk in two populations. *Diabetologia* 2001;44(3):333–339.

17. **Petersson U, Ostgren CJ, Brudin L, Brismar K, Nilsson PM.** Low levels of insulin-like growth-factor-binding protein-1 (IGFBP-1) are prospectively associated with the incidence of type 2 diabetes and impaired glucose tolerance (IGT): the Söderåkra Cardiovascular Risk Factor Study. *Diabetes Metab.* 2009;35(3):198–205.

18. **Lewitt MS, Hilding A, Ostenson C-G, Efendic S, Brismar K, Hall K.** Insulin-like growth factor-binding protein-1 in the prediction and development of type 2 diabetes in middle-aged Swedish men. *Diabetologia* 2008;51(7):1135–1145.

19. **Lewitt MS, Hilding A, Brismar K, Efendic S, Ostenson C-G, Hall K.** IGF-binding protein 1 and abdominal obesity in the development of type 2 diabetes in women. *Eur. J. Endocrinol.* 2010;163(2):233–242.

20. **Haywood NJ, Cordell PA, Tang KY, Makova N, Yuldasheva NY, Imrie H, Viswambharan H, Bruns AF, Cubbon RM, Kearney MT, Wheatcroft SB.** Insulin-Like Growth Factor Binding Protein 1 Could Improve Glucose Regulation and Insulin Sensitivity Through Its RGD Domain. *Diabetes* 2017;66(2):287–299.

21. **Laughlin GA, Barrett-Connor E, Criqui MH, Kritz-Silverstein D.** The prospective association of serum insulin-like growth factor I (IGF-I) and IGF-binding protein-1 levels with all cause and cardiovascular disease mortality in older adults: the Rancho Bernardo Study. *J. Clin. Endocrinol. Metab.* 2004;89(1):114–120.

22. **Mellbin LG, Rydén L, Brismar K, Morgenthaler NG, Ohrvik J, Catrina SB.** Copeptin, IGFBP-1, and cardiovascular prognosis in patients with type 2 diabetes and acute myocardial infarction: a report from the DIGAMI 2 trial. *Diabetes Care* 2010;33(7):1604–1606.

23. **Wallander M, Norhammar A, Malmberg K, Ohrvik J, Rydén L, Brismar K.** IGF binding protein 1 predicts cardiovascular morbidity and mortality in patients with acute myocardial infarction and type 2 diabetes. *Diabetes Care* 2007;30(9):2343–2348.

24. **Rajwani A, Ezzat V, Smith J, Yuldasheva NY, Duncan ER, Gage M, Cubbon RM, Kahn MB, Imrie H, Abbas A, Viswambharan H, Aziz A, Sukumar P, Vidal-Puig A, Sethi JK, Xuan S, Shah AM, Grant PJ, Porter KE, Kearney MT, Wheatcroft SB.** Increasing circulating IGFBP1 levels improves insulin sensitivity, promotes nitric oxide production, lowers blood pressure, and protects against atherosclerosis. *Diabetes* 2012;61(4):915–924.

25. **Accili D, Drago J, Lee EJ, Johnson MD, Cool MH, Salvatore P, Asico LD, José PA, Taylor SI, Westphal H.** Early neonatal death in mice homozygous for a null allele of the insulin receptor gene. *Nat. Genet.* 1996;12(1):106–109.

26. **Crossey PA, Jones JS, Miell JP.** Dysregulation of the insulin/IGF binding protein-1 axis in transgenic mice is associated with hyperinsulinemia and glucose intolerance. *Diabetes* 2000;49(3):457–465.

27. **Wheatcroft SB, Shah AM, Li J-M, Duncan E, Noronha BT, Crossey PA, Kearney MT.** Preserved glucoregulation but attenuation of the vascular actions of insulin in mice heterozygous for knockout of the insulin receptor. *Diabetes* 2004;53(10):2645–2652.

28. **Rode B, Shi J, Endesh N, Drinkhill MJ, Webster PJ, Lotteau SJ, Bailey MA, Yuldasheva NY, Ludlow MJ, Cubbon RM, Li J, Futers TS, Morley L, Gaunt HJ, Marszalek K, Viswambharan H, Cuthbertson K, Baxter PD, Foster R, Sukumar P, Weightman A, Calaghan SC, Wheatcroft SB, Kearney MT, Beech DJ.** Piezo1 channels sense whole body physical activity to reset cardiovascular homeostasis and enhance performance. *Nat. Commun.* 2017;8(1):350.

29. **Porter KE, Naik J, Turner NA, Dickinson T, Thompson MM, London NJM.** Simvastatin inhibits human saphenous vein neointima formation via inhibition of smooth muscle cell proliferation and migration. *J. Vasc. Surg.* 2002;36(1):150–157.

30. **Imrie H, Abbas A, Viswambharan H, Rajwani A, Cubbon RM, Gage M, Kahn M, Ezzat VA, Duncan ER, Grant PJ, Ajjan R, Wheatcroft SB, Kearney MT.** Vascular insulin-like growth factor-I resistance and diet-induced obesity. *Endocrinology* 2009;150(10):4575–4582.

31. **Boudaoud A, Burian A, Borowska-Wykręt D, Uyttewaal M, Wrzalik R, Kwiatkowska D, Hamant O.** FibrilTool, an ImageJ plug-in to quantify fibrillar structures in raw microscopy images. *Nat. Protoc.* 2014;9(2):457–463.

32. **Hynes RO.** Integrins: versatility, modulation, and signaling in cell adhesion. *Cell* 1992;69(1):11–25.

33. **Shen T-L, Park AY-J, Alcaraz A, Peng X, Jang I, Koni P, Flavell RA, Gu H, Guan J-L.** Conditional knockout of focal adhesion kinase in endothelial cells reveals its role in angiogenesis and vascular development in late embryogenesis. *J. Cell Biol.* 2005;169(6):941–952.

34. **van Nieuw Amerongen GP, Koolwijk P, Versteilen A, van Hinsbergh VWM.** Involvement of RhoA/Rho kinase signaling in VEGF-induced endothelial cell migration and angiogenesis in vitro. *Arterioscler. Thromb. Vasc. Biol.* 2003;23(2):211–217.

35. **Cubbon RM, Kahn MB, Wheatcroft SB.** Effects of insulin resistance on endothelial progenitor cells and vascular repair. *Clin. Sci. Lond. Engl. 1979* 2009;117(5):173–190.

36. **Hagensen MK, Raarup MK, Mortensen MB, Thim T, Nyengaard JR, Falk E, Bentzon JF.** Circulating endothelial progenitor cells do not contribute to regeneration of endothelium after murine arterial injury. *Cardiovasc. Res.* 2012;93(2):223–231.

37. **Tsuzuki M.** Bone marrow-derived cells are not involved in reendothelialized endothelium as endothelial cells after simple endothelial denudation in mice. *Basic Res. Cardiol.* 2009;104(5):601–611.

38. **Lindner V, Reidy MA, Fingerle J.** Regrowth of arterial endothelium. Denudation with minimal trauma leads to complete endothelial cell regrowth. *Lab. Investig. J. Tech. Methods Pathol.* 1989;61(5):556–563.

39. **Borai A, Livingstone C, Ferns G.** Reference change values for insulin and insulin-like growth factor binding protein-1 (IGFBP-1) in individuals with varying degrees of glucose tolerance. *Scand. J. Clin. Lab. Invest.* 2013;73(4):274–278.

40. **Gleeson LM, Chakraborty C, McKinnon T, Lala PK.** Insulin-like growth factor-binding protein 1 stimulates human trophoblast migration by signaling through alpha 5 beta 1 integrin via mitogen-activated protein Kinase pathway. *J. Clin. Endocrinol. Metab.* 2001;86(6):2484–2493.

41. **Perks CM, Newcomb PV, Norman MR, Holly JM.** Effect of insulin-like growth factor binding protein-1 on integrin signalling and the induction of apoptosis in human breast cancer cells. *J. Mol. Endocrinol.* 1999;22(2):141–150.

42. **Ammoun S, Schmid MC, Zhou L, Ristic N, Ercolano E, Hilton DA, Perks CM, Hanemann CO.** Insulin-like growth factor-binding protein-1 (IGFBP-1) regulates human schwannoma proliferation, adhesion and survival. *Oncogene* 2012;31(13):1710–1722.

43. **Lee H-J, Lee J-S, Hwang SJ, Lee H-Y.** Insulin-like growth factor binding protein-3 inhibits cell adhesion via suppression of integrin β4 expression. *Oncotarget* 2015;6(17):15150–15163.

44. **Margadant C, Monsuur HN, Norman JC, Sonnenberg A.** Mechanisms of integrin activation and trafficking. *Curr. Opin. Cell Biol.* 2011;23(5):607–614.

45. **López-Marure R, Bernal AE, Zentella A.** Interference with c-myc expression and RB phosphorylation during TNF-mediated growth arrest in human endothelial cells. *Biochem. Biophys. Res. Commun.* 1997;236(3):819–824.

46. **Krasinski K, Spyridopoulos I, Kearney M, Losordo DW.** In vivo blockade of tumor necrosis factor-alpha accelerates functional endothelial recovery after balloon angioplasty. *Circulation* 2001;104(15):1754–1756.

47. **Hanks SK, Calalb MB, Harper MC, Patel SK.** Focal adhesion protein-tyrosine kinase phosphorylated in response to cell attachment to fibronectin. *Proc. Natl. Acad. Sci. U. S. A.* 1992;89(18):8487–8491.

48. **Juliano RL.** Signal transduction by cell adhesion receptors and the cytoskeleton: functions of integrins, cadherins, selectins, and immunoglobulin-superfamily members. *Annu. Rev. Pharmacol. Toxicol.* 2002;42:283–323.

49. **Zhao X, Guan J-L.** Focal adhesion kinase and its signaling pathways in cell migration and angiogenesis. *Adv. Drug Deliv. Rev.* 2011;63(8):610–615.

50. **Chang E, Heo K-S, Woo C-H, Lee H, Le N-T, Thomas TN, Fujiwara K, Abe J.** MK2 SUMOylation regulates actin filament remodeling and subsequent migration in endothelial cells by inhibiting MK2 kinase and HSP27 phosphorylation. *Blood* 2011;117(8):2527–2537.

Table & Figure Legends

Figure 1 - Endothelial regeneration after wire injury of the femoral artery. IGFBP-1 rescues endothelial regeneration in insulin resistant mice.

A: Representative *in situ* Evans blue staining 5 days after vascular injury (blue staining indicates denuded endothelium) in WT, IGFBP1-tg, $IR^{+/-}$ and $IR^{+/-}$IGFBP1-tg mice (magnification ×20).

B: Endothelial regeneration 5 days after vascular injury in WT and IGFBP-1tg mice (*n* = 7 mice per group). No significant difference was seen between WT and IGFBP-1tg mice.

C. Endothelial regeneration 5 days post-vascular wire injury, in WT, $IR^{+/-}$ and $IR^{+/-}$IGFBP1-tg mice (*n* = 5-10 per group). **P* < 0.05, **P<0.01

Figure 2 - Progenitor Cell Abundance and Function.

A-C: Enumeration of myeloid angiogenic cells (MAC) derived from blood, spleen, and bone marrow by cell culture after 7 days. Numbers of peripheral blood (**A**) (n=5-6), spleen (**B**) (n=6)- and bone marrow (**C**) (n=6-9)-derived cultured MACs from uninjured mice are shown. * P < 0.05. HPF=high power field

D. Adhesion capacity of spleen-derived MACs expressed as number of cells adhering to fibronectin-coated plates (*n* = 5-6). No significant difference between groups was observed.

E. Enumeration of circulating $Sca\text{-}1^{+}/Flk\text{-}1^{+}$ cells. Number of $Sca\text{-}1^{+}/Flk\text{-}1^{+}$ cells were quantified in peripheral blood by flow cytometry. No significant difference between groups was identified. (n=6).

Figure 3 - hIGFBP1 improves adhesion of human endothelial cells to denuded human saphenous vein and upregulates cell-surface integrins.

A-B: Representative images of cell-tracker labelled human coronary artery endothelial cells adherent to denuded saphenous vein after pre-incubation with control medium (**A**) or hIGFBP1 (500ng/mL) (**B**) for 60 minutes. (Magnification - x10).

C: Significantly more cells were adherent to the saphenous vein after pre-incubation with hIGFBP1 (500ng/mL 60 mins). (n=5) *** P<0.001.

D: Adhesion of human coronary artery endothelial cells to glass cover slips. Human coronary artery endothelial cells were incubated in 1%FCS +/-hIGFBP1 (500ng/mL) for indicated times before fixing cells with paraformaldehyde and staining with H&E. Adherent cells were quantified in 10 random fields at x400 magnification. There were no significant differences between control and hIGFBP1-treated cells at each time point.

E-F: Cell-surface integrin expression. Human coronary artery endothelial cells were incubated +/- hIGFBP1 (500ng/mL) for one hour before quantification of cell-surface integrins using an integrin-mediated cell adhesion array kit (Millipore, MA, USA). Expression of α-integrins (**E**) and β-integrins (**F**) are indicated. (n=6). *P<0.05; **P<0.01.

Figure 4 – hIGFBP1 abrogates TNF-α-induced inhibition of endothelial cell migration

A-B: No significant difference in migration in response to hIGFBP1 (500ng/mL 48h) was observed in HUVECs (**A**) or HCAECs (**B**) in a Scratch wound healing assay. (n=3).

C-D: Pre-incubation with TNF-α (10ng/mL) for the indicated times inhibited insulin-stimulated (100nmol/L 15 mins) Akt phosphorylation in HUVECs. Representative immunoblot (**C**) and mean data of pAkt/Akt ratio (**D**) are shown.

E-F: hIGFBP1 (500ng/mL) partially restored endothelial migratory responses following exposure to TNF-α (10mg/mL) in scratch wound assays. **E:** HUVECs (n=9) *p< 0.01) **F:** HCAECs (n=6). *P<0.05.

Figure 5 - IGFBP-1 does not act as chemotactic agent for endothelial cell migration in Boyden chamber assays.

A Effect of hIGFBP1 (500ng/mL 6h) on migration in HUVECs, (n=3), no significant difference was seen

B Effect of hIGFBP1 (500ng/mL 6h) on migration in HCAECs (n=5), P=0.07

C Effects of IGFBP-1 (500ng/mL 6h) and VEGF (50ng/mL 6h) on cell migration (HCAECs), (n=5), Control v. VEGF ** P<0.01, VEGF v. VEGF+IGFBP-1 – no significant difference.

Figure 6 - hIGFBP1 improves endothelial cell proliferation in a pro-inflammatory setting.

A HUVEC proliferation. Quiesced cells treated with 2.5% FCS supplemented with insulin (100 nmol/L) or hIGFBP1 (500ng/mL). Cells counted after 5 days with insulin or hIGFBP1 treatment. (*n*=4), *p<0.05.

B HCAEC proliferation. Quiesced cells treated with 20% FCS supplemented with either vehicle or 500ng/mL hIGFBP1. Cells counted after 5 days with control or hIGFBP1 treatment. (*n*=4).

C Concentration-dependent effect of TNF-α on inhibition of proliferation in HCAECS. Cells counted after 5 days following TNF-α treatment (0.01-10ng/mL) (n=3)

D HCAEC proliferation. Quiesced cells treated with 20% FCS supplemented with TNF-α (1ng/mL), hIGFBP1 (500ng/mL) or a combination of TNF-α (1ng/mL) and IGFBP-1 (500ng/mL). Cells counted after 5 days. ANOVA: P<0.01. Post hoc: **P <0.01, *P <0.05 (*n*=6).

Figure 7 – IGF-independent effects of hIGFBP1 and involvement its RGD domain and focal adhesion kinase on endothelial cell proliferation.

A: hIGFBP1 [500ng/L] and IGF-1 [18nM] both independently stimulated proliferation of HUVEC in an EdU assay. There was no additive effect of IGF-1 and hIGFBP1 on cell proliferation.

B&C: Wild-type hIGFBP1 stimulated proliferation of HUVEC. Proliferation was not significantly increased by hIGFBP1 when the RGD domain was mutated to WGD.

D: The positive effect of hIGFBP1 on proliferation of HUVEC was abrogated by the focal adhesion kinase inhibitor (FAK-i) PZ0117 (100 nmol/L) (n=4) *P < 0.05 NS=not significant

Figure 8- hIGFBP1 stimulates phosphorylation of focal adhesion kinase, activates the small GTPase Rho A and ameliorates TNF-α induced cytoskeletal rearrangement in endothelial cells

A-B: hIGFBP1 (500ng/mL 15mins) induced rapid ^{397}Tyr phosphorylation of focal adhesion kinase (FAK) in HUVEC. A: representative immunoblot. B: mean data of pFAK/FAK ratio. (n=6) *P<0.05. C-D. Mutation of the RGD domain of IGFBP1 to WGD (incapable of integrin-binding) abrogates phosphorylation of FAK. C: representative immunoblot. D. mean data of pFAK/FAK ratio (n=6). E. hIGFBP1 (500ng/mL) induced time-dependent activation of Rho A in HCAECs. (n=5) **P<0.01. F-G: effects of TNF-α (10ng/mL) and hIGFBP1 (500ng/mL) on actin fibre anisotropy in HUVECs F: representative images (scale bar represents 100 µm). G: mean data from four repeat experiments with 188-287 cells per experiment *P<0.05, **P<0.01

Antibody Table

List of antibodies used, manufacturer, catalogue number and research resource identifier (RRID).

Figures & Tables

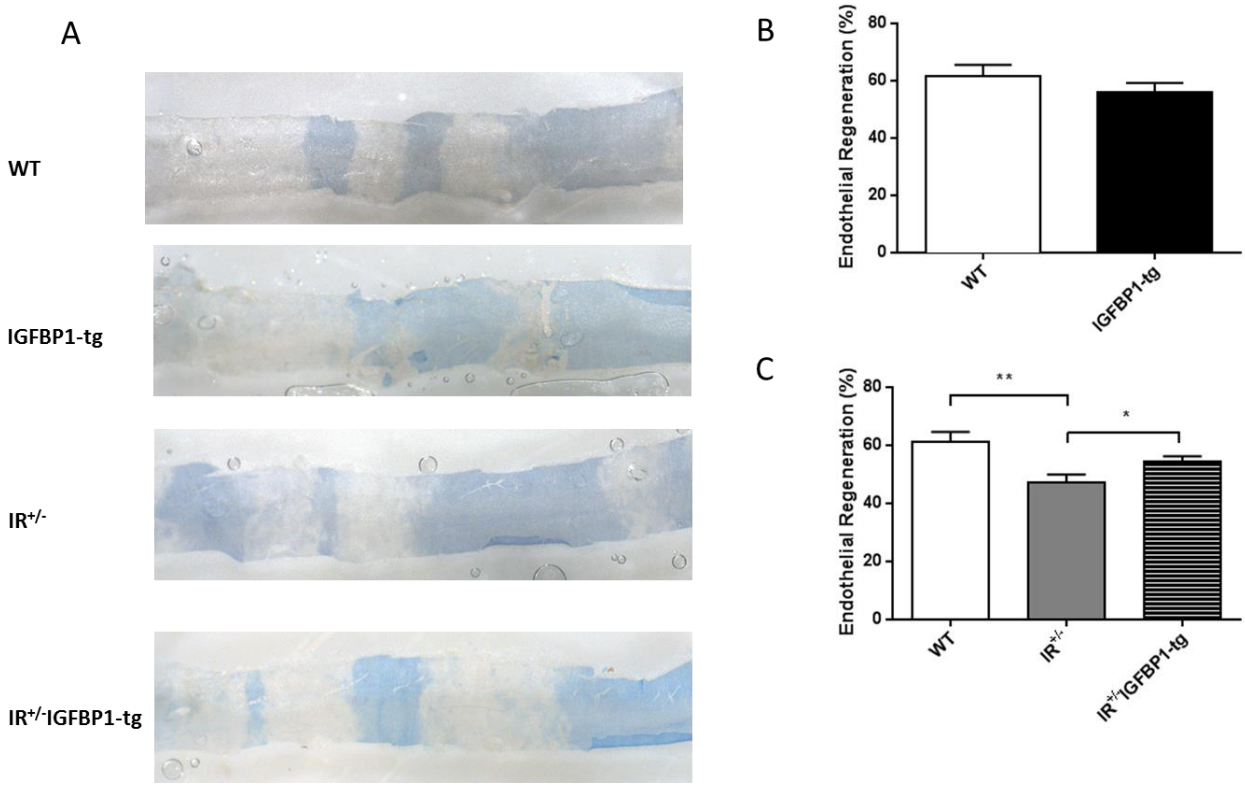

Figure 1 - Endothelial regeneration after wire injury of the femoral artery. IGFBP-1 rescues endothelial regeneration in insulin resistant mice.

A: Representative *in situ* Evans blue staining 5 days after vascular injury (blue staining indicates denuded endothelium) in WT, IGFBP1-tg, $IR^{+/-}$ and $IR^{+/-}$IGFBP1-tg mice (magnification ×20).

B: Endothelial regeneration 5 days after vascular injury in WT and IGFBP-1tg mice (*n* = 7 mice per group). No significant difference was seen between WT and IGFBP-1tg mice.

C. Endothelial regeneration 5 days post-vascular wire injury, in WT, $IR^{+/-}$ and $IR^{+/-}$IGFBP1-tg mice (*n* = 5-10 per group). **P* < 0.05, **P<0.01

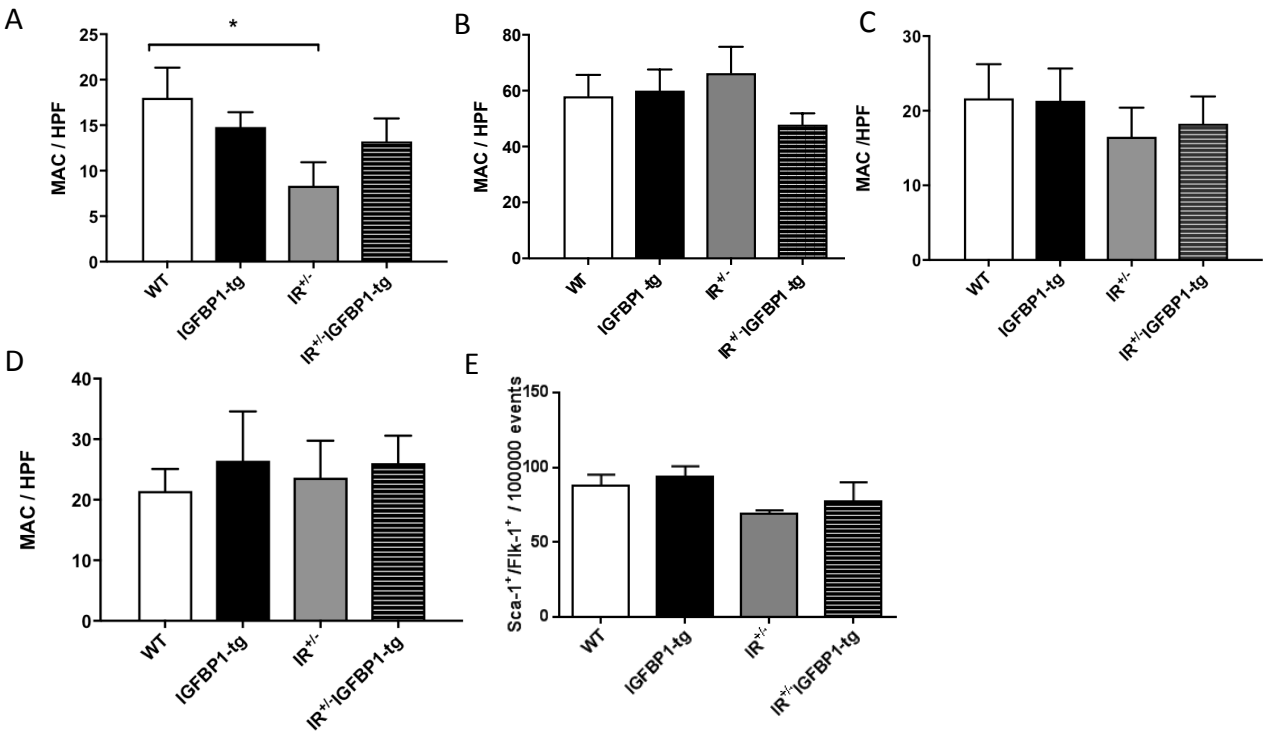

Figure 2 - Progenitor Cell Abundance and Function.

A-C: Enumeration of myeloid angiogenic cells (MAC) derived from blood, spleen, and bone marrow by cell culture after 7 days. Numbers of peripheral blood (**A**) (n=5-6), spleen (**B**) (n=6)- and bone marrow (**C**) (n=6-9)-derived cultured MACs from uninjured mice are shown. * $P < 0.05$. HPF=high power field

D. Adhesion capacity of spleen-derived MACs expressed as number of cells adhering to fibronectin-coated plates (*n* = 5-6). No significant difference between groups was observed.

E. Enumeration of circulating Sca-1^+/Flk-1^+ cells. Number of Sca-1^+/Flk-1^+ cells were quantified in peripheral blood by flow cytometry. No significant difference between groups was identified. (n=6).

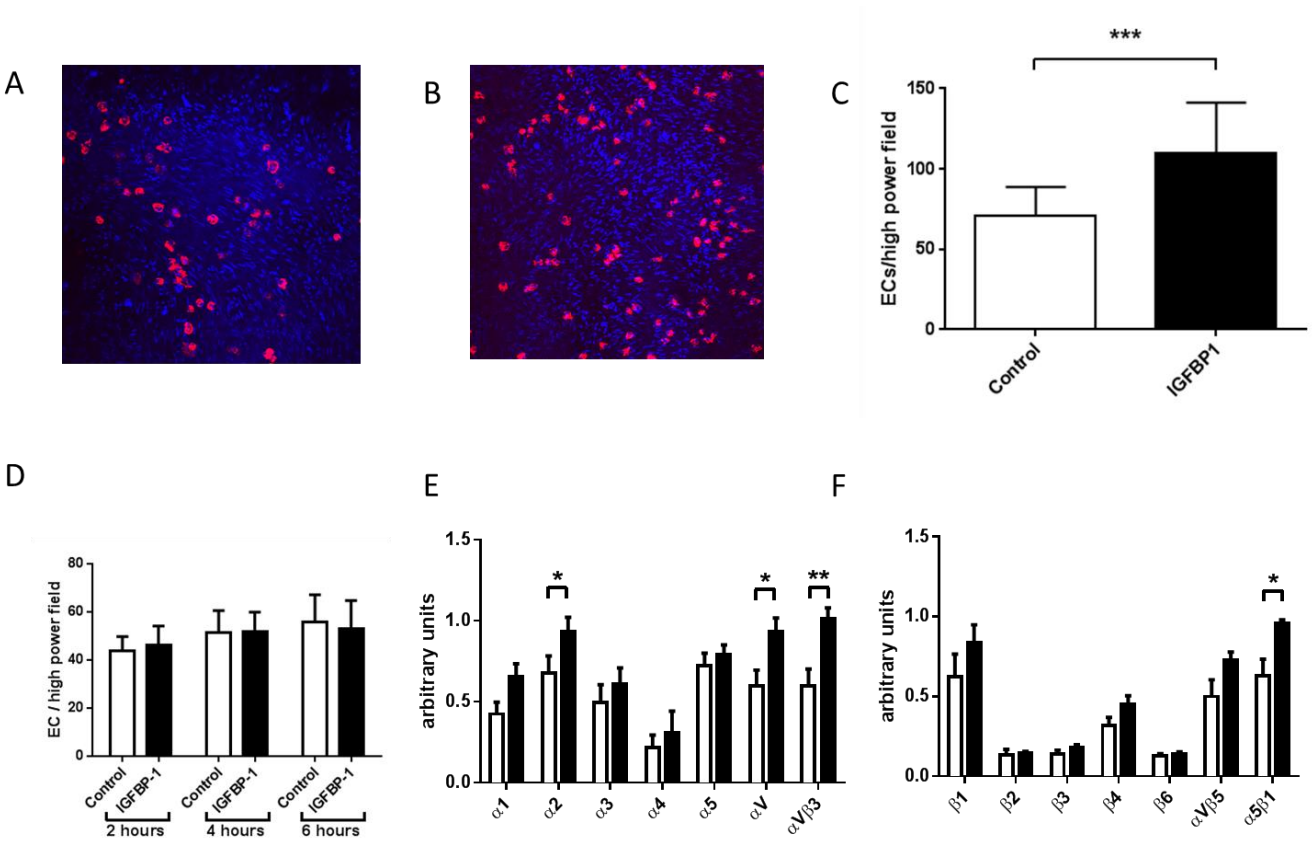

Figure 3 - hIGFBP1 improves adhesion of human endothelial cells to denuded human saphenous vein and upregulates cell-surface integrins.

A-B: Representative images of cell-tracker labelled human coronary artery endothelial cells adherent to denuded saphenous vein after pre-incubation with control medium (**A**) or hIGFBP1 (500ng/mL) (**B**) for 60 minutes. (Magnification - x10).

C: Significantly more cells were adherent to the saphenous vein after pre-incubation with hIGFBP1 (500ng/mL 60 mins). (n=5) *** P<0.001.

D: Adhesion of human coronary artery endothelial cells to glass cover slips. Human coronary artery endothelial cells were incubated in 1%FCS +/-hIGFBP1 (500ng/mL) for indicated times before fixing cells with paraformaldehyde and staining with H&E. Adherent cells were quantified in 10 random fields at x400 magnification. There were no significant differences between control and hIGFBP1-treated cells at each time point.

E-F: Cell-surface integrin expression. Human coronary artery endothelial cells were incubated +/- hIGFBP1 (500ng/mL) for one hour before quantification of cell-surface integrins using an integrin-mediated cell adhesion array kit (Millipore, MA, USA). Expression of α-integrins (**E**) and β-integrins (**F**) are indicated. (n=6). *P<0.05; **P<0.01.

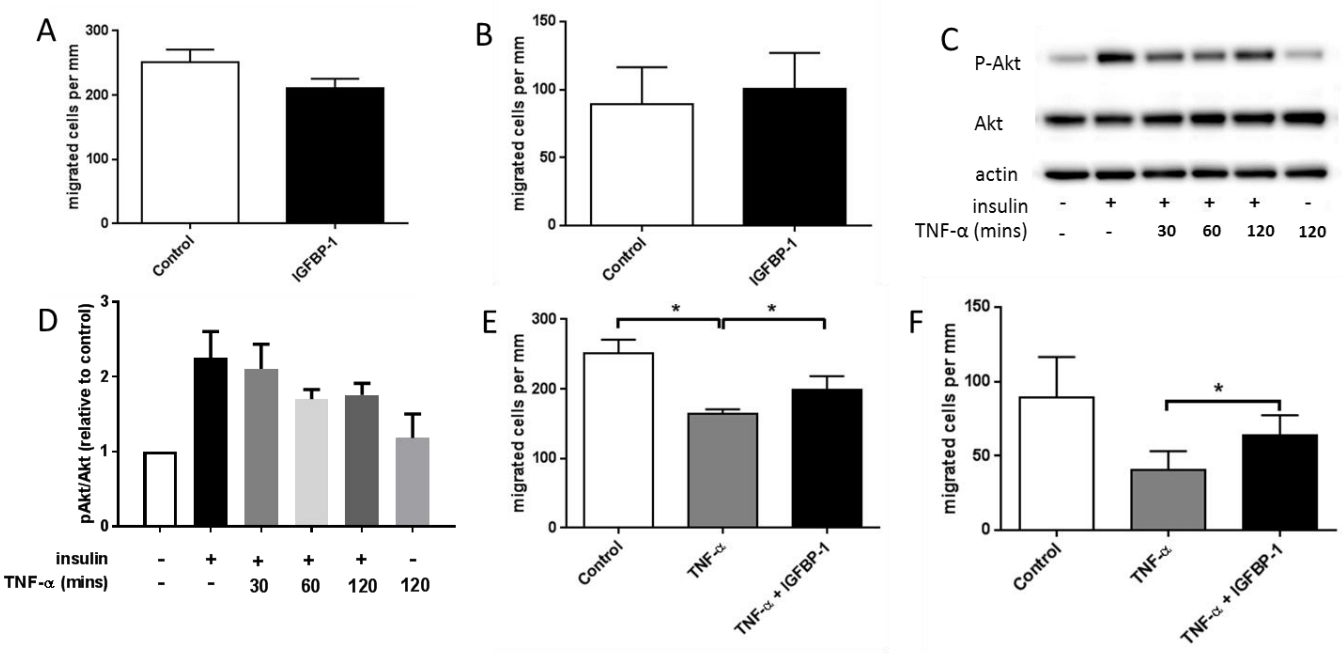

871

872 **Figure 4 – hIGFBP1 abrogates TNF-α-induced inhibition of endothelial cell migration**

873 **A-B:** No significant difference in migration in response to hIGFBP1 (500ng/mL 48h) was
874 observed in HUVECs (**A**) or HCAECs (**B**) in a Scratch wound healing assay. (n=3).**C-D:**
875 Pre-incubation with TNF-α (10ng/mL) for the indicated times inhibited insulin-stimulated
876 (100nmol/L 15 mins) Akt phosphorylation in HUVECs. Representative immunoblot (**C**) and
877 mean data of pAkt/Akt ratio (**D**) are shown. **E-F:** hIGFBP1 (500ng/mL) partially restored
878 endothelial migratory responses following exposure to TNF-α (10mg/mL) in scratch wound
879 assays. **E:** HUVECs (n=9) *p< 0.01) **F:** HCAECs (n=6). *P<0.05.

880

881

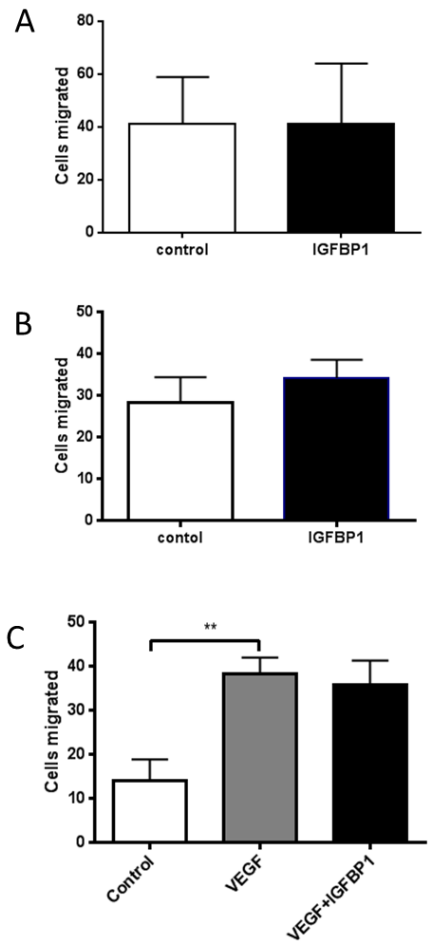

Figure 5 - IGFBP-1 does not act as chemotactic agent for endothelial cell migration in Boyden chamber assays.

A Effect of hIGFBP1 (500ng/mL 6h) on migration in HUVECs, (n=3), no significant difference was seen

B Effect of hIGFBP1 (500ng/mL 6h) on migration in HCAECs (n=5), P=0.07

C Effects of IGFBP-1 (500ng/mL 6h) and VEGF (50ng/mL 6h) on cell migration (HCAECs), (n=5), Control v. VEGF ** P<0.01, VEGF v. VEGF+IGFBP-1 – no significant difference.

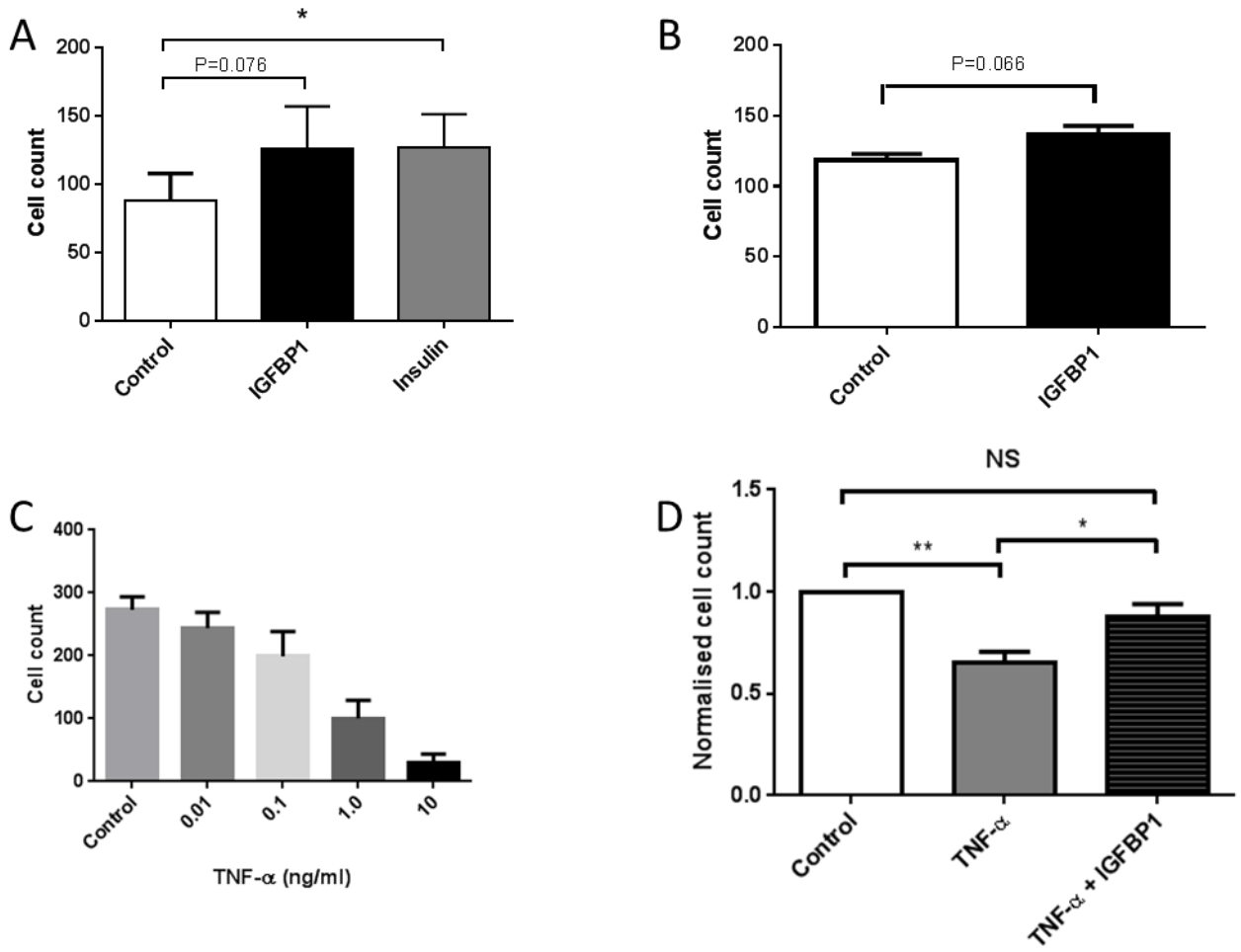

Figure 6 - hIGFBP1 improves endothelial cell proliferation in a pro-inflammatory setting.

A HUVEC proliferation. Quiesced cells treated with 2.5% FCS supplemented with insulin (100 nmol/L) or hIGFBP1 (500ng/mL). Cells counted after 5 days with insulin or hIGFBP1 treatment. (*n*=4), *p<0.05.

B HCAEC proliferation. Quiesced cells treated with 20% FCS supplemented with either vehicle or 500ng/mL hIGFBP1. Cells counted after 5 days with control or hIGFBP1 treatment. (*n*=4).

C Concentration-dependent effect of TNF-α on inhibition of proliferation in HCAECS. Cells counted after 5 days following TNF-α treatment (0.01-10ng/mL) (n=3)

D HCAEC proliferation. Quiesced cells treated with 20% FCS supplemented with TNF-α (1ng/mL), hIGFBP1 (500ng/mL) or a combination of TNF-α (1ng/mL) and IGFBP-1 (500ng/mL). Cells counted after 5 days. ANOVA: P<0.01. Post hoc: **P <0.01, *P <0.05 (*n*=6).

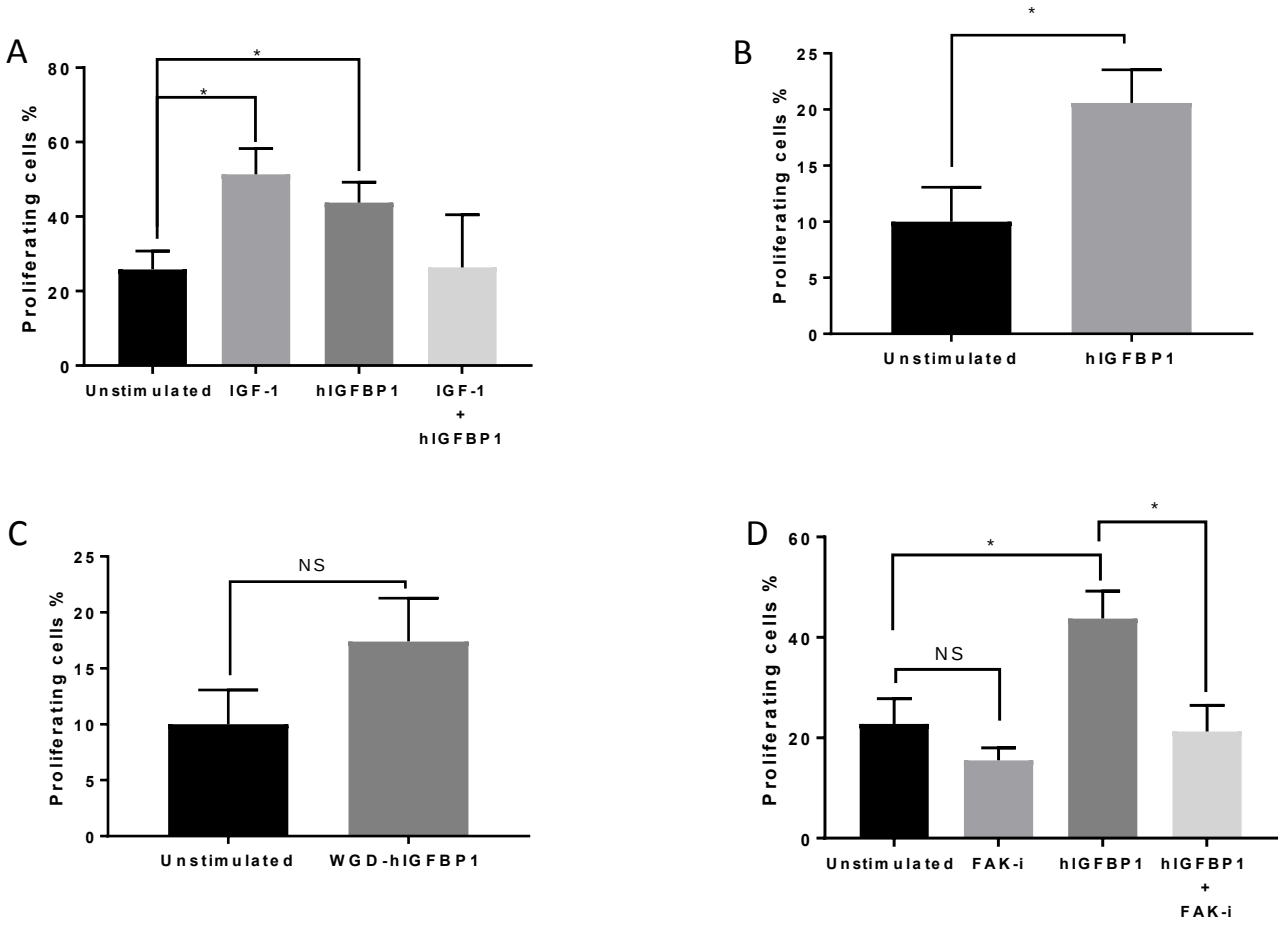

910 **Figure 7 – IGF-independent effects of hIGFBP1 and involvement its RGD domain and**
911 **focal adhesion kinase on endothelial cell proliferation.**

912 **A:** hIGFBP1 [500ng/L] and IGF-1 [18nM] both independently stimulated proliferation of
913 HUVEC in an EdU assay. There was no additive effect of IGF-1 and hIGFBP1 on cell
914 proliferation. **B&C:** Wild-type hIGFBP1 stimulated proliferation of HUVEC. Proliferation was
915 not significantly increased by hIGFBP1 when the RGD domain was mutated to WGD. **D:** The
916 positive effect of hIGFBP1 on proliferation of HUVEC was abrogated by the focal adhesion
917 kinase inhibitor (FAK-i) PZ0117 (100 nmol/L) (n=4) *$P < 0.05$ NS=not significant

918

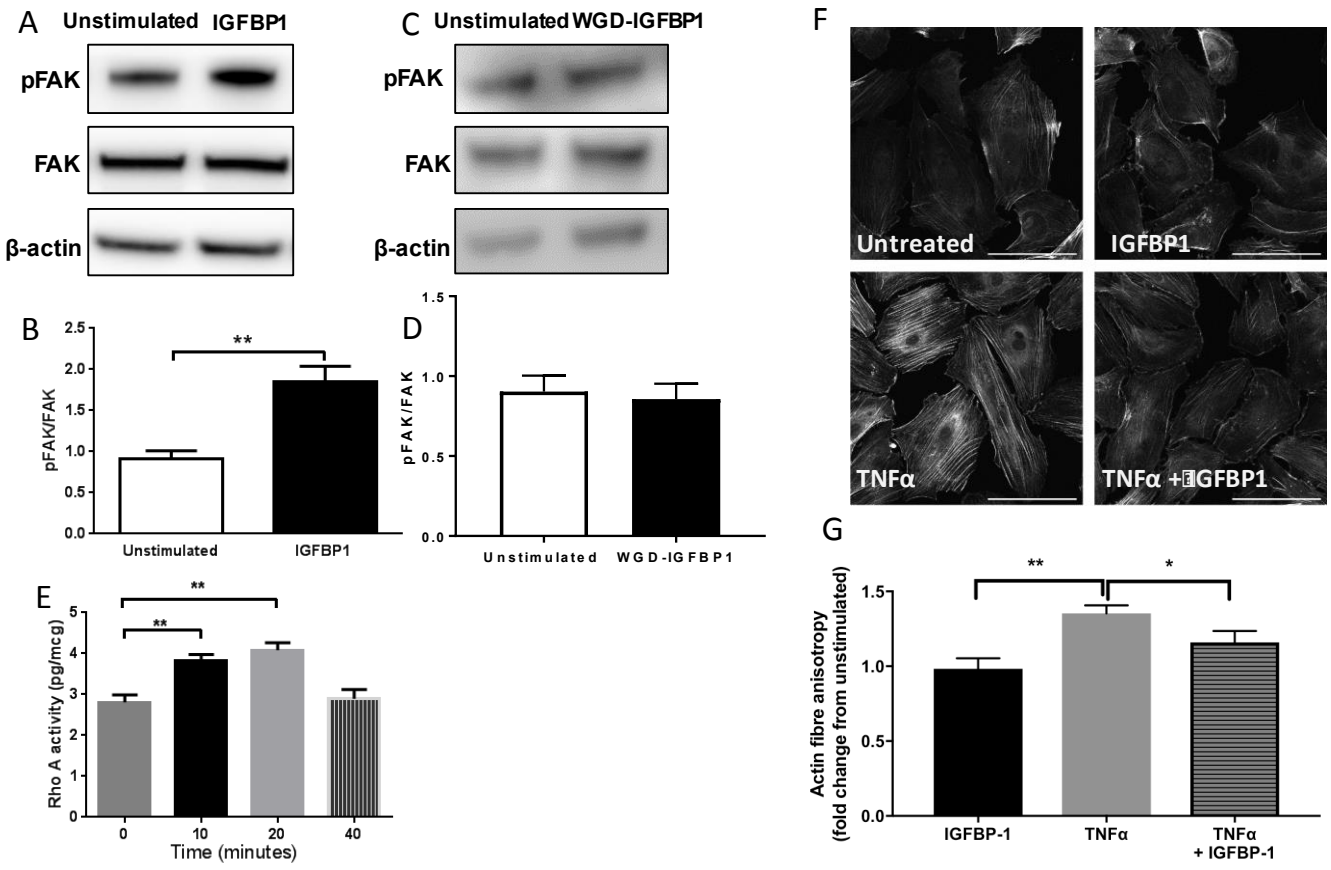

Figure 8- hIGFBP1 stimulates phosphorylation of focal adhesion kinase, activates the small GTPase Rho A and ameliorates TNF-α induced cytoskeletal rearrangement in endothelial cells

A-B: hIGFBP1 (500ng/mL 15mins) induced rapid ^{397}Tyr phosphorylation of focal adhesion kinase (FAK) in HUVEC. A: representative immunoblot. B: mean data of pFAK/FAK ratio. (n=6) *P<0.05. C-D. Mutation of the RGD domain of IGFBP1 to WGD (incapable of integrin-binding) abrogates phosphorylation of FAK. C: representative immunoblot. D. mean data of pFAK/FAK ratio (n=6). E. hIGFBP1 (500ng/mL) induced time-dependent activation of Rho A in HCAECs. (n=5) **P<0.01. F-G: effects of TNF-α (10ng/mL) and hIGFBP1 (500ng/mL) on actin fibre anisotropy in HUVECs F: representative images (scale bar represents 100 μm). G: mean data from four repeat experiments with 188-287 cells per experiment *P<0.05, **P<0.01

Antibody Table

Peptide/Protein target	Name of antibody	Manufacturer, catalogue #	RRID	Species raised, monoclonal or polyclonal	Dilution
Sca-1	FITC Rat Anti-Mouse Ly-6A/E	BD Pharmingen, 557405	AB_396688	Rat, monoclonal	1:5000
Rat IgG2a isotype control	FITC Rat IgG2a, κ Isotype Control	BD Pharmingen, 553929	AB_395144	Rat, monoclonal	1:5000
Flk-1	PE Rat Anti-Mouse Flk-1	BD Pharmingen, 561052	AB_2034023	Rat, monoclonal	1:5000
Rat IgG2a isotype control	PE Rat IgG2a, κ Isotype Control	BD Pharmingen, 553930	RRID:AB_479719	Rat, monoclonal	1:5000
CD16/CD32	Mouse BD Fc Block	BD Pharmingen, 553152	AB_398533	Rat, monoclonal	1:10
Akt	Akt	Cell Signaling, 9272	AB_329827	Rabbit, polyclonal	1:1000
pAkt	Phospho-Akt (Ser473) (D9E) XP	Cell Signaling, 4060	AB_2315049	Rabbit, monoclonal	1:2000
FAK	Focal adhesion kinase	Cell Signaling, 3285	AB_2269034	Rabbit, polyclonal	1:20 000
pFAK	Phospho-FAK (Tyr397) (D20B1)	Cell Signaling, 8556	AB_10891442	Rabbit, monoclonal	1:2000
β-actin	β-actin antibody (C4)	Santa Cruz Sc-47778	AB_626632	Mouse, monoclonal	1:1000

951 **Supplementary Figures**

952

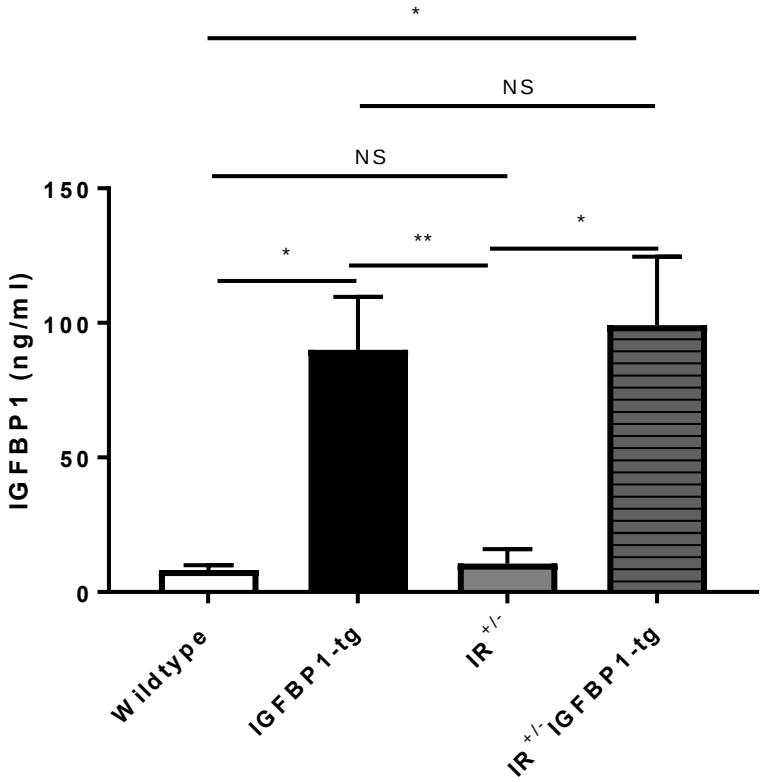

953

954 **Supplementary Figure 1 – Plasma concentration of IGFBP1 in mice.** Plasma IGFBP1
955 level was measured by ELISA in wild type mice, mice heterozygous for deletion of the insulin
956 receptor ($IR^{+/-}$) and IGFBP1 transgenic (-tg) mice. (n=6-15) *P < 0.05, **P<0.01, NS=not
957 significant.

958

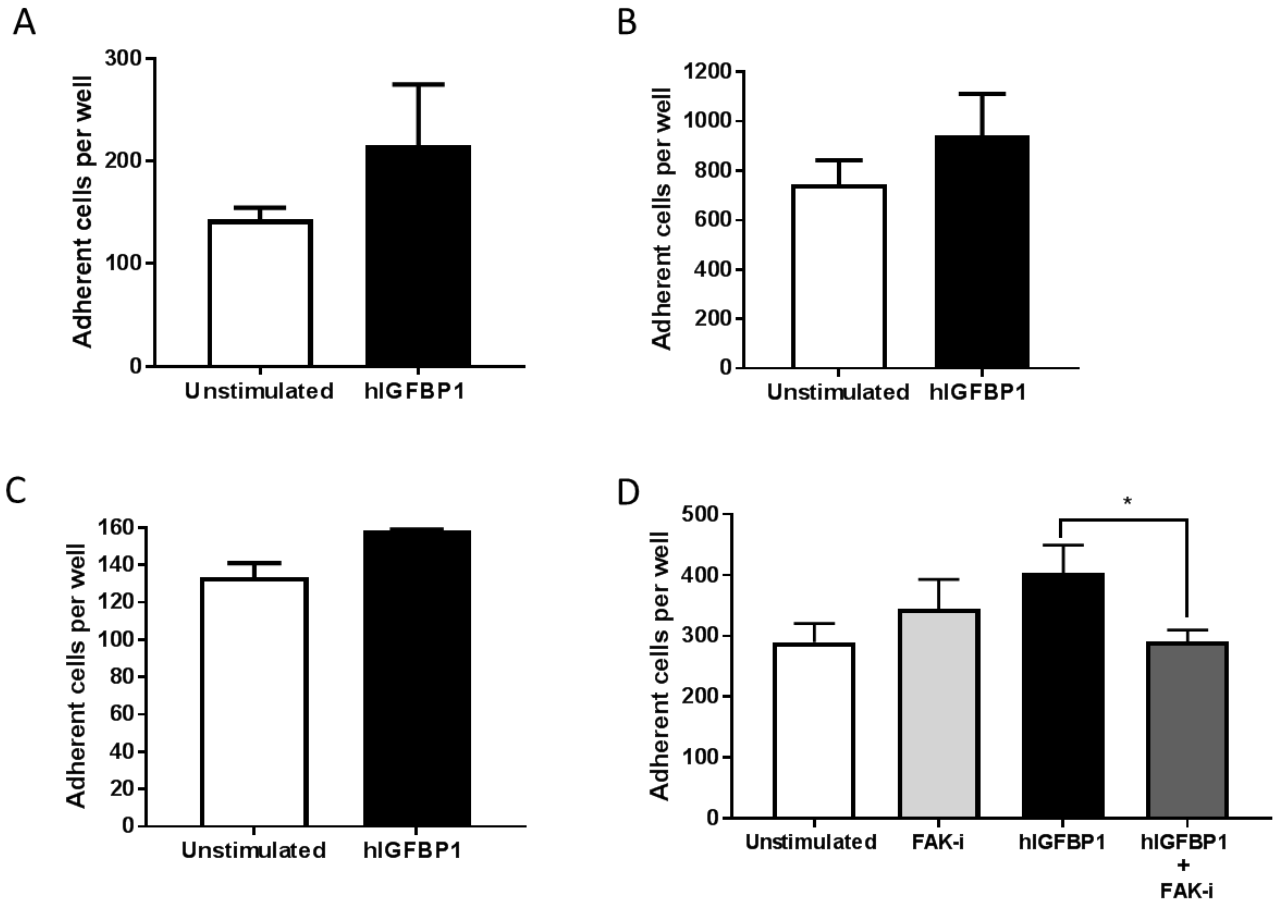

959

960

961 **Supplementary Figure 2** – **Effects of hIGFBP1 on adhesion of endothelial cells to**
962 **extracellular matrix constituents**. HUVEC were incubated with hIGFBP1 (500ng/mL 60
963 mins) before quantifying adhesion to the following matrix components: **A**: fibronectin; **B**:
964 collagen I; **C**: vitronectin; **D**: collagen IV. There was a non-specific trend to increased
965 adhesion in response to hIGFBP1 but none of the effects on adhesion to individual
966 components reached statistical significance. Inhibition of focal adhesion kinase (FAK-i) did
967 not influence the adhesion of unstimulated cells (**D**). Adhesion to collagen IV in the presence
968 of hIGFBP1 was significantly reduced by inhibition of focal adhesion kinase (**D)** (n=4-8)
969 $P<0.05$.
970

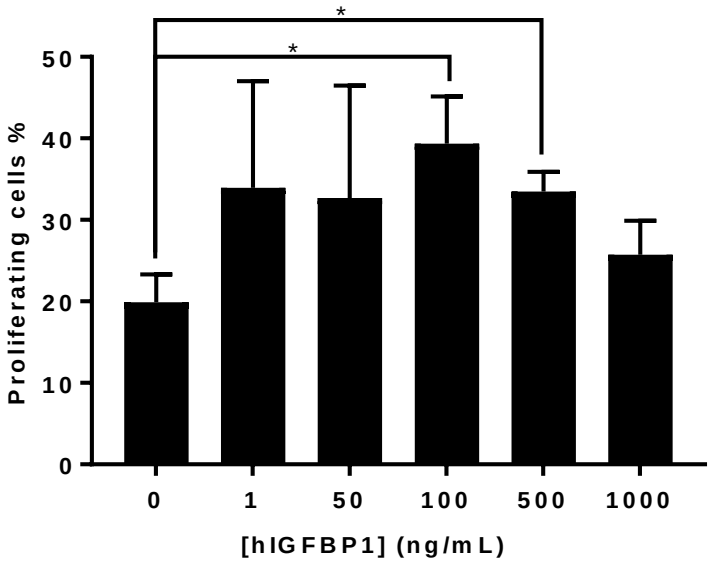

971

972 **Supplementary Figure 3 – Concentration-dependence of hIGFBP1-stimulated**
973 **endothelial cell proliferation.**

974 HUVEC proliferation was quantified with an EdU assay after incubation with hIGFBP1 at the
975 indicated concentrations. Stimulation of proliferation by hIGFBP1 reached statistical
976 significance at 100-500ng/mL (n=3) *$P < 0.05$

977